

Multi-Rate Nyquist-SCM for C-Band 100Gbit/s Signal over 50km Dispersion-Uncompensated Link

Haide Wang, Ji Zhou, Jinlong Wei, Dong Guo, Yuanhua Feng, Weiping Liu, Changyuan Yu, Dawei Wang, and Zhaohui Li

Abstract—In this paper, to the best of our knowledge, we propose the first multi-rate Nyquist-subcarriers modulation (SCM) for C-band 100Gbit/s signal transmission over 50km dispersion-uncompensated link. Chromatic dispersion (CD) introduces severe spectral nulls on optical double-sideband signal, which greatly degrades the performance of intensity-modulation and direct-detection systems. In the previous works, high-complexity digital signal processing (DSP) is required to resist the CD-caused spectral nulls. Based on the characteristics of dispersive channel, Nyquist-SCM with multi-rate subcarriers is proposed to keep away from the CD-caused spectral nulls flexibly. Signal on each subcarrier can be individually recovered by a DSP with an acceptable complexity, including the feed-forward equalizer with no more than 31 taps, a two-tap post filter, and maximum likelihood sequence estimation with one memory length. Combining with entropy loading based on probabilistic constellation shaping to maximize the capacity-reach, the C-band 100Gbit/s multi-rate Nyquist-SCM signal over 50km dispersion-uncompensated link can achieve 7% hard-decision forward error correction limit and average normalized generalized mutual information of 0.967. In conclusion, the multi-rate Nyquist-SCM shows great potentials in solving the CD-caused spectral distortions.

Index Terms—Intensity-modulation and direct-detection systems, chromatic dispersion, multi-rate Nyquist-SCM, probabilistic constellation shaping.

I. INTRODUCTION

IN recent years, network applications such as 4K/8K high-definition television, augmented reality/virtual reality, and edge cloud computing are driving the growth of the global data traffics [1]. To satisfy the ever-increasing capacity demands, high-speed intensity-modulation and direct-detection (IM/DD)

optical systems have been paid much attentions, which keep the advantages of low cost, low power consumption and small footprint [2]–[4]. However, compared to the O-band IM/DD optical systems, those operating at C-band with relative low link loss are facing with much more severe power fading challenge caused by chromatic dispersion (CD) [5]–[7].

In order to eliminate distortions caused by CD, dispersion-compensation module (DCM) is commonly used [8], [9]. However, DCM not only complicates the link configuration, but also increases the link loss. In addition, the complex modulation schemes have drawn much more attention for resisting CD, which mainly include optical single-sideband (SSB) modulation [10], and CD pre-compensation [11]. IM and coherent detection can be also used for CD compensation [12]. However, these schemes require either more complicated transmitters or the receivers compared to IM/DD optical communications. For optical double-sideband (DSB) signal, the advanced digital signal processing (DSP) can be effectively to solve the problems caused by CD. However, high-complexity DSP algorithms are required to resist CD-caused spectral nulls, including the decision feedback equalizer [13], Tomlinson-Harashima pre-coding [14], and maximum likelihood sequence estimation (MLSE) with relatively long memory length [15], [16]. Discrete multi-tone (DMT) with bit and power loading has a CD resistance but its peak-to-average power ratio (PAPR) is relatively high [17], [18].

Recently, the optical SSB Nyquist-subcarriers modulation (SCM) has attracted much attention because of the strong CD resistance, high spectral efficiency and lower PAPR compared to DMT [19], [20]. Although the optical SSB signal is robust against CD-caused power fading, half of the power is lost due to one sideband suppression and extra devices are required for the optical SSB signal generation compared to the optical DSB signal. In this paper, an optical DSB multi-rate Nyquist-SCM with multi-rate subcarriers is proposed to keep away from the CD-caused spectral nulls flexibly. Therefore, the signal of each subcarrier can be recovered individually by low complexity adaptive channel-matched detection (ACMD) algorithm [21], including the feed-forward equalizer (FFE) with no more than 31 taps, a two-tap post filter (PF) and MLSE with one memory length. Moreover, by combining entropy loading based on probabilistic constellation shaping (PCS) with SCM, it can maximize the capacity-reach [22]. To the best of our knowledge, we propose the first multi-rate Nyquist-SCM for C-band 100Gbit/s IM/DD optical signal transmission over 50km dispersion-uncompensated link.

The main contributions of this paper are as follows:

- The multi-rate Nyquist-SCM system is proposed, which

Manuscript received; revised. This work was supported in part by National Key R&D Program of China (2019YFB1803500); National Natural Science Foundation of China (62005102, U2001601); Natural Science Foundation of Guangdong Province (2019A1515011059); Guangzhou Basic and Applied Basic Research Foundation (202102020996); Fundamental Research Funds for the Central Universities (21619309); Open Fund of IPOC (BUPT) (IPOC2019A001). (Corresponding authors: Ji Zhou)

H. Wang, J. Zhou, Y. Feng and W. Liu are with Department of Electronic Engineering, College of Information Science and Technology, Jinan University, Guangzhou 510632, China (e-mail: 1834041007@stu2018.jnu.edu.cn; zhouji@jnu.edu.cn; favinfeng@163.com; wpl@jnu.edu.cn).

J. Wei is with Huawei Technologies Duesseldorf GmbH, European Research Center, Germany (e-mail:jnlongwei2@huawei.com).

D. Guo is with School of Information and Electronics, Beijing Institute of Technology, Beijing 100081, China (e-mail: 7520190141@bit.edu.cn).

C. Yu is with the Department of Electronic and Information Engineering, The Hong Kong Polytechnic University, Hong Kong (e-mail: changyuan.yu@polyu.edu.hk).

D. Wei and Z. Li are with the Guangdong Provincial Key Laboratory of Optoelectronic Information Processing Chips and Systems, Sun Yat-sen University, Guangzhou 510275, China. Also with the State Key Laboratory of Optoelectronic Materials and Technologies. And also with the Southern Marine Science and Engineering Guangdong Laboratory (Zhuhai), 519000, China (e-mail: wangdw9@mail.sysu.edu.cn, lzhh88@mail.sysu.edu.cn).

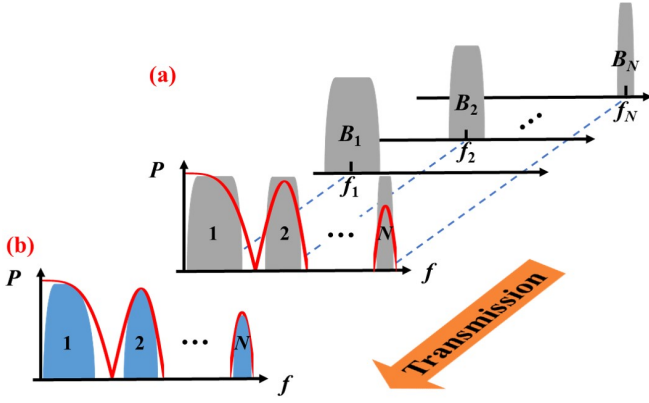


Fig. 1. The spectrum for the multi-rate Nyquist-SCM signal at (a) the transmitter side and (b) the receiver side, respectively.

successfully combines the advanced technologies of Nyquist-SCM, multi-rate subcarriers, ACMD algorithm and the entropy loading based on PCS.

- To the best of our knowledge, we present the first C-band 100Gbit/s IM/DD optical multi-rate Nyquist-SCM transmission over a 50km dispersion-uncompensated link achieving 7% hard-decision forward error correction (HD-FEC) limit and average normalized generalized mutual information (NGMI) of 0.967.

The remainder of the paper is organized as follows. In Section II, the principle of the proposed multi-rate Nyquist-SCM system is given. In Section III, the experimental setups of C-band 100Gbit/s IM/DD optical multi-rate Nyquist-SCM system over 50km dispersion-uncompensated link are presented. The experimental results and discussions are demonstrated in Section IV. Finally, the paper is concluded in Section V.

II. PRINCIPLE OF MULTI-RATE NYQUIST-SCM SYSTEM

After the square-law detection, the frequency response of fiber dispersive channel can be expressed as [23]

$$H(f) = \cos(2\pi^2\beta_2 L f^2) \quad (1)$$

where β_2 is group velocity coefficient and L is the fiber length. This CD-caused power fading will result in spectral nulls in signal spectrum [24]. Fig. 1 shows the schematic diagram of the spectrum for the multi-rate Nyquist-SCM signal at (a) the transmitter side and (b) the receiver side, respectively. Due to limited bandwidth of devices and the CD of the fiber link, the frequency response of the channel is a cosine function with an overall downward trend as the red line shown in Fig. 1. The multi-rate Nyquist-SCM signal contains N frequency-domain bands with different bandwidths. After up-conversion and Nyquist shaping, the intermediate frequency (IF) of i^{th} band signal is f_i and the bandwidth is B_i , where $i = 1, 2, \dots, N$. Based on the characteristics of dispersive channel, the proposed multi-rate Nyquist-SCM system can flexibly adjust the band count, bandwidth and IF of each band to keep away from the CD-caused spectral nulls. After the transmission, each band signal does not suffer from the CD-caused spectral nulls. Therefore, the proposed multi-rate Nyquist-SCM system naturally has a strong resistance to CD.

Further, modulation formats with different modulation order or entropy can be adopted to make full use of the signal-to-noise ratio (SNR) of each band to maximize the capacity-reach.

Figure 2 shows DSP of the N -band multi-rate Nyquist-SCM system at (a) the transmitter side and (b) the receiver side. The multi-rate Nyquist-SCM signals can be generated digitally by the transmitter side DSP. N tributaries bits can be mapped to the uniform or PCS quadrature amplitude modulation (QAM) symbols with different entropy to make full use of the SNR. For the i^{th} band, the real part R_i and the imaginary part I_i of the M_i -ary QAM symbol are up-sampled and filtered by square-root raised cosine (RRC) filters to realize the up-sampling and Nyquist-shaping. The impulse response $g_i(n)$ of the i^{th} band RRC filter can be expressed as

$$g_i(n) = \frac{\sin \pi(1 - \beta_i)n/T_i + 4\beta_i n/T_i \cdot \cos \pi(1 + \beta_i)n/T_i}{\pi n/T_i \cdot [1 - (4\beta_i n/T_i)^2]}, \quad (2)$$

where T_i is the duration of the symbols, β_i is the filter roll-off factor. A N -band multi-rate Nyquist-SCM system requires $2N$ shaping filters at the transmitter side and $2N$ matched filters at the receiver side for in-phase (I) and quadrature (Q) components.

After applying pulse shaping, the signal is resampled to baud rate of RS_i . Then digital up converters (DUC) at the transmitter side shift baseband signal to the IF of f_i Hz ($i = 1, 2, \dots, N$). For the i^{th} band, bandwidth B_i of IF signal is

$$B_i = (1 + \beta_i) \times RS_i. \quad (3)$$

After DUC, the pulse shaped IF signals of all bands are combined and the transmitted signal can be expressed as

$$\begin{aligned} s(n) &= \sum_{i=1}^N s_{I,i}(n) + s_{Q,i}(n) \\ &= \sum_{i=1}^N \sum_k \left[R_{i,k} g_i \left(n - \frac{k}{F_s} \right) \cos 2\pi f_i \left(n - \frac{k}{F_s} \right) \right. \\ &\quad \left. + I_{i,k} g_i \left(n - \frac{k}{F_s} \right) \sin 2\pi f_i \left(n - \frac{k}{F_s} \right) \right] \end{aligned} \quad (4)$$

where F_s is the sampling frequency. Then the transmitted signal $s(n)$ is reconstructed to analog signal $s(t)$ by digital-to-analog converters (DAC) for digital-to-analog (D/A) conversion. After the electrical-to-optical (E/O) conversion, the optical transmitted signals are uploaded into the fiber.

At the receiver side, the electrical IF signal after O/E conversion at each band is shifted to the baseband by the digital down converters (DDC). After being resampled, the baseband received signals are filtered by a matched filter with impulse response $g_i(-n)$. The output of the DDC in I and Q channel can be expressed as

$$\begin{aligned} m_{I,i}(n) &= \sum_k [s(t) \otimes h(t) + z(t)] \Big|_{t=\frac{k}{F_s}} \\ &\quad \times g_i \left(-n + \frac{k}{F_s} \right) \cos 2\pi f_i \left(n - \frac{k}{F_s} \right), \end{aligned} \quad (5)$$

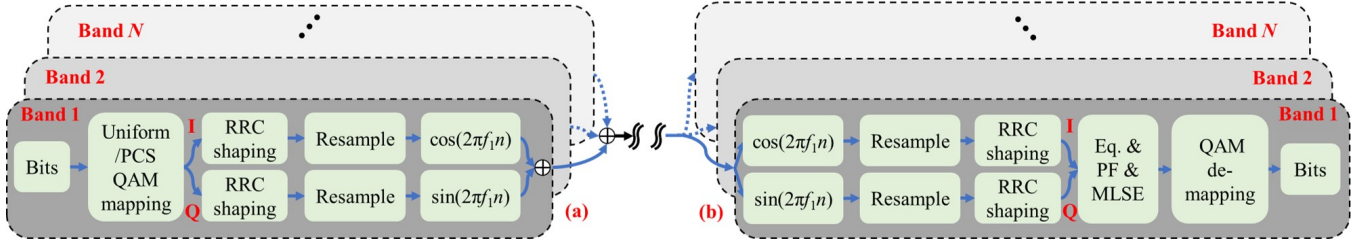


Fig. 2. DSP of the N -band multi-rate Nyquist-SCM system at (a) the transmitter side and (b) the receiver side.

$$m_{Q,i}(n) = \sum_k [s(t) \otimes h(t) + z(t)] \Big|_{t=\frac{k}{F_s}} \times g_i \left(-n + \frac{k}{F_s} \right) \sin 2\pi f_i \left(n - \frac{k}{F_s} \right), \quad (6)$$

where $h(t)$ is the impulse response of the channel and \otimes is convolution. $z(t)$ is the noise. For the I (Q) component at the i^{th} band, the cross-channel interference from the Q (I) component is filtered out by low pass RRC matched filter. As a result, the output of the matched filter in I and Q channel are proportion to the real part R_i and imaginary part I_i of M_i -ary QAM symbol, respectively. The output of the matched filter can be expressed as

$$y_{I,i}(n) \propto \frac{1}{2} \times R_{i,k} \otimes h(t) + z'(t) \Big|_{t=\frac{n}{F_s}}, \quad (7)$$

$$y_{Q,i}(n) \propto \frac{1}{2} \times I_{i,k} \otimes h(t) + z'(t) \Big|_{t=\frac{n}{F_s}} \quad (8)$$

where $z'(t)$ denotes the noise $z(t)$ after the processing of DDC and matched filters.

After down sampling, the received real part $y_{I,i}(n)$ and imaginary part $y_{Q,i}(n)$ signal make up the M_i -ary QAM symbol for equalization. The output of the complex signal FFE can be expressed as

$$q_i(n) = \sum_{k=0}^{L-1} \omega_k^* \times [y_{I,i}(n-k) + jy_{Q,i}(n-k)] \quad (9)$$

where ω is the tap coefficients of the L -tap FFE and $(\cdot)^*$ is the complex conjugate. Tap coefficients of FFE are trained by least mean square (LMS) algorithm. At the j^{th} iteration, the tap coefficients of the FFE are updated by

$$\omega_k(j) = \omega_k(j-1) - 2 \times \mu \times g(j-1) \quad (10)$$

where μ ($0 < \mu < 1$) is the step size and the gradient $g(j)$ is

$$g(j) = \sum_{k=0}^{L-1} [q_i(j) - d_i(j)]^* \times [y_{I,i}(j-k) + jy_{Q,i}(j-k)] \quad (11)$$

where d_i is the transmitted signal at the i^{th} band. After the training process, the tap coefficients are tracked by decision

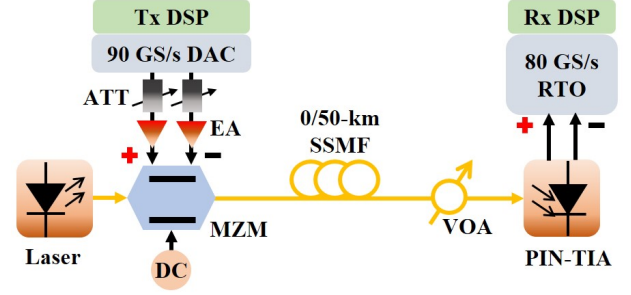


Fig. 3. The experimental setups of C-band 100Gbit/s IM/DD optical multi-rate Nyquist-SCM system transmission over dispersion-uncompensated links.

directed-LMS (DD-LMS) algorithm. The gradient $g(j)$ is calculated as

$$g(j) = \sum_{k=0}^{L-1} [q_i(j) - \hat{q}_i(j)]^* \times [y_{I,i}(j-k) + jy_{Q,i}(j-k)] \quad (12)$$

where \hat{q}_i is the decision of q_i . The training-based equalizer is also expected to eliminate the cycle slip issue [25].

However, the in-band noise will be amplified inevitably after equalization, which can be solve by the ACMD algorithm. A two-tap PF can be used to suppress the noise but introduces a known inter-symbol interference (ISI). The output of the i^{th} band PF is

$$p_i(n) = q_i(n) + \alpha \times q_i(n-1) \quad (13)$$

where α is the tap coefficient of the PF. The known ISI can be eliminated by MLSE with one memory length. Finally, the M_i -ary QAM symbol is de-mapped to the bits.

III. EXPERIMENTAL SETUPS

The experimental setups of C-band 100Gbit/s IM/DD optical multi-rate Nyquist-SCM system over dispersion-uncompensated links is shown in Fig. 3. First of all, a 64Gbit/s on-off keying preamble was used for channel estimate to determine the channel nulls positions. The band count of the multi-rate Nyquist-SCM system transmission over 50km standard single-mode fiber (SSMF) was 7. There were 378260 bits divided into 7 tributaries for generating the multi-rate Nyquist-SCM, which was designed based on the channel information estimated by the preamble. The IF f_i of each band was set to 3.9, 12, 17.3, 21.3, 24.5, 27.4 and 29.95GHz, respectively. And the rate RS_i was set to 7.01, 5.11, 3.81,

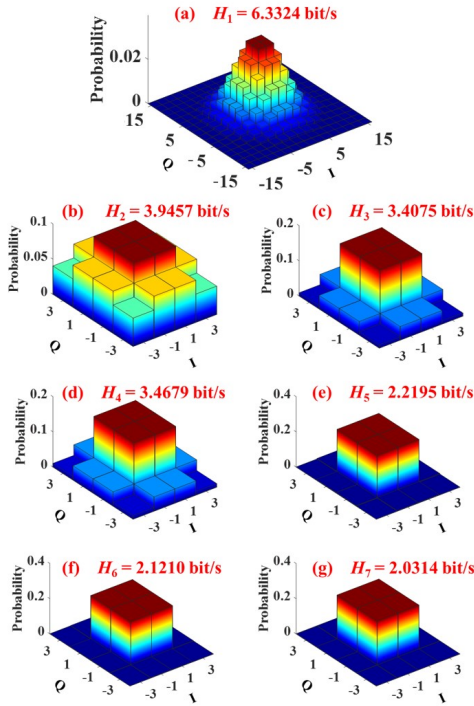


Fig. 4. The probability of the constellation points of the PCS QAM adopted by each band.

2.76, 2.9, 2.62 and 1.92GBaud, respectively. In addition, roll-off factor β_i of the RRC filter was set to 0.1 for the first three bands and 0.01 for the rest four bands, respectively.

After DSP at the transmitter side as shown in Fig. 2(a), the frame was uploaded into DAC with resolution of 8 bit, 90GSa/s sampling rate and 16GHz 3dB bandwidth. After being amplified by the electrical amplifiers (EA, Centellax OA4SMM4) followed the 6-dB attenuators (ATT), a 40Gbps Mach-Zehnder modulator (MZM, Fujitsu FTM7937EZ) @ push-pull mode with two differential inputs was used to modulate the amplified multi-rate Nyquist-SCM signal on a continuous wave optical carrier at 1550.02nm for generating optical DSB multi-rate Nyquist-SCM signal. A 2.3V direct current (DC) bias was applied on the MZM. The generated optical multi-rate Nyquist-SCM signal was fed into the 0/50km SSMF, respectively. The launch optical power was set to 6.56dBm (i.e., the maximum launch optical power of the device). The maximum received optical power (ROP) was approximately -4 dBm and total link loss was approximately 10.66dB over 50km SSMF transmission.

At the receiver side, a variable optical attenuator (VOA) was used to adjust the ROP. Then optical multi-rate Nyquist-SCM signal was converted into an electrical signal by a 31GHz P-type-intrinsic-N-type diode with trans impedance amplifier (PIN-TIA, Finisar MPRV1331A). The differential electrical signal was fed into a 80GSa/s real-time oscilloscope (RTO) with cut-off bandwidth of 36GHz to implement A/D conversion. The digital multi-rate Nyquist-SCM signal was decoded by off-line processing, including resampling, synchronization, multi-rate Nyquist-SCM signal decoding as shown in Fig. 2(b) and bit error rate (BER) calculation.

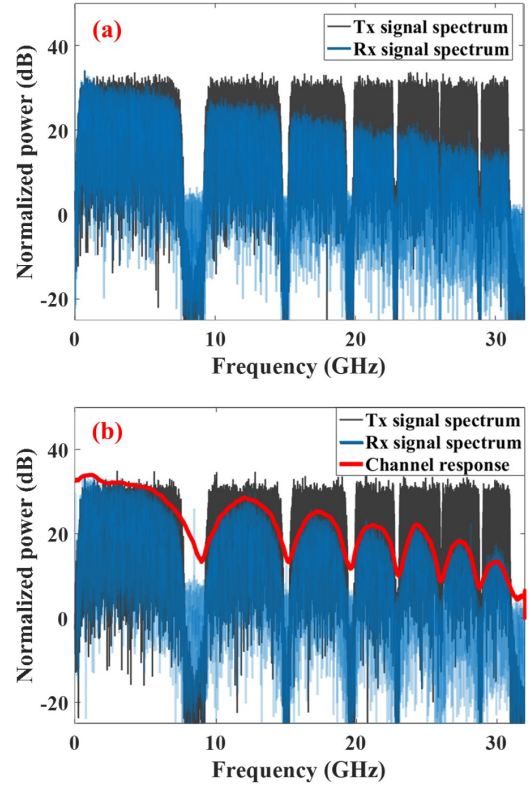


Fig. 5. Electrical frequency spectrum of the transmitted signal and received signal of the 100Gbit/s multi-rate Nyquist-SCM system over (a) OBTB transmission and (b) 50km SSMF transmission and the estimated channel response.

IV. EXPERIMENTAL RESULTS AND DISCUSSION

Due to the limited bandwidth, the capacity of bands in high frequency are lower than those close to the low frequency. The uniform QAM with different order and PCS QAM with different entropy are used respectively. When the uniform QAM is adopted, 128QAM, 16QAM, 8QAM, 8QAM, 4QAM, 4QAM and binary phase shift keying is used for the band from 1st to 7th, respectively. The link rate is 102.18Gbit/s. Based on the PCS with constant composition distribution matching, the QAM formats with various probabilistic distributions for entropy loading are allocated to each band of the proposed multi-rate Nyquist-SCM system to make full use of the SNR. When the PCS QAM is adopted, PCS 256QAM is used for 1st band and PCS 16QAM with different entropy are used for the rest bands. Figs. 4(a)-(g) show the probability of the constellation points of the PCS QAM adopted by each band, respectively. The entropy are also attached. In such case, the link rate is about 103Gbit/s.

Figure 5 shows the electrical frequency spectrum of the transmitted signal and received signal of the 100Gbit/s multi-rate Nyquist-SCM system over (a) optical back-to-back (OBTB) and (b) 50km SSMF transmission and the estimated channel response. The transmitted 100Gbit/s multi-rate Nyquist-SCM signal is well-designed based on the estimated channel response to keep away from the CD-caused spectral nulls. The total bandwidth of the multi-rate Nyquist-SCM signal is approximately 31GHz. As the Fig. 5(a) shows, there

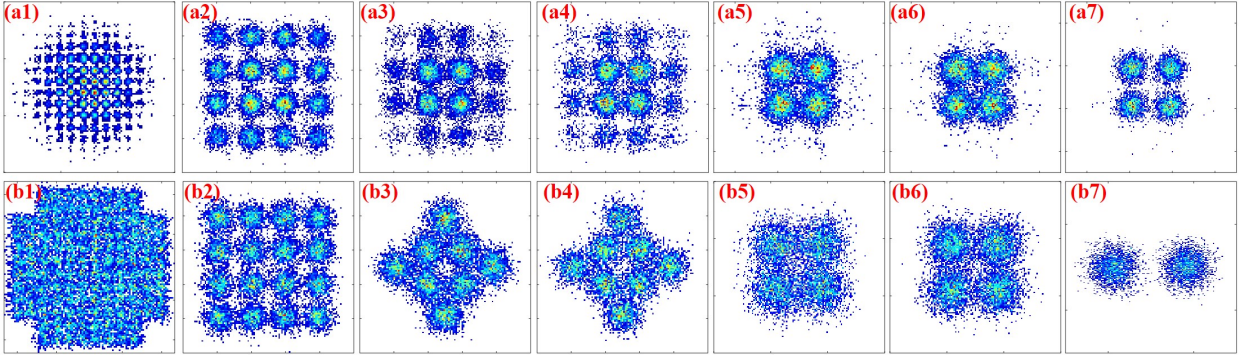


Fig. 6. Constellations of the equalized signal over 50km SSMF transmission at ROP of approximately -4 dBm adopting (a1)-(a7) the PCS QAM and (b1)-(b7) the uniform QAM of each band.

is only the limited bandwidth that causes the power fading of the received signal for the OBTB transmission scenario. After 50km SSMF transmission, the received signal suffers from power fading caused by both limited bandwidth and CD as shown in Fig. 5(b). Fortunately, the multi-rate Nyquist-SCM signal keeps away from the 7 spectral nulls caused by CD. Therefore, the proposed multi-rate Nyquist-SCM has a strong resistance to CD and a FFE with no more than 31 taps can equalize the signal without the use of complicated DSP technology.

Constellations of the equalized signal over 50km SSMF transmission at ROP of approximately -4 dBm adopting the PCS QAM and the uniform QAM of each band are shown in Fig. 6. As shown in Figs. 6(a1)-(a7), when the PCS QAM scheme is adopted, the occurrence probabilities of the outer constellation points are lower than those of the inner constellation points. When the uniform QAM scheme is adopted, the occurrence probabilities of the constellation points are approximately the same as shown in Figs. 6(b1)-(b7). Whether uniform QAM or PCS QAM modulation scheme is adopted, the signal of each band is equalized after FFE processing. The tap numbers of FFEs are set to 31 for the first two bands and 21 for the rest five bands, respectively. The step sizes of LMS algorithm for training are all set to 5×10^{-3} and those of DD-LMS algorithm for tracking are all set to 10^{-3} . The lengths of training sequence for these 7 bands are set to 500, 300, 300, 300, 200, 200 and 100, respectively. After deducting training overhead, the data rates are about 100.377Gbit/s and 100.301Gbit/s for PCS QAM and uniform QAM, respectively.

Figure 7 shows the BER performance versus ROPs for 100Gbit/s IM/DD optical multi-rate Nyquist-SCM system. Power fading is the main factor that limits the system performance. Compared to the spectrum of signal after OBTB transmission as shown in Fig. 5, after 50km SSMF transmission, not only the limited bandwidth of the devices, but the CD also results in signal power fading. As a result, the BER performance of the 100Gbit/s IM/DD optical multi-rate Nyquist-SCM system over 50km SSMF transmission is worse than that over OBTB transmission, whether uniform QAM or PCS QAM modulation scheme is adopted. For the OBTB transmission scenario, when the ROP is greater than approximately -5.8 dBm for the uniform QAM modulation

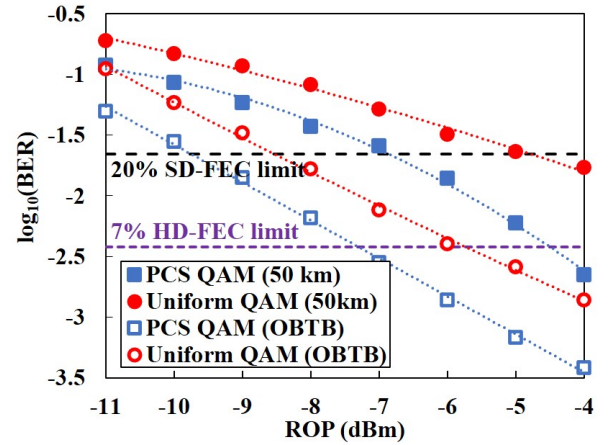


Fig. 7. BER performance versus ROPs for 100Gbit/s IM/DD optical multi-rate Nyquist-SCM system adopting the uniform QAM and PCS QAM schemes over OBTB and 50km SSMF transmission, respectively.

scheme, BER achieves to be below the 7% HD-FEC limit (i.e., 3.8×10^{-3}). If the PCS QAM modulation scheme is employed, BER can achieve to be below 7% HD-FEC limit when ROP is greater than approximately -7.2 dBm. For the 50km SSMF transmission scenario, when the ROP is greater than approximately -4.8 dBm for the uniform QAM modulation scheme, BER can only achieve to be below the 20% soft-decision FEC (SD-FEC) limit (i.e., 2.2×10^{-2}). If PCS QAM modulation scheme is utilized, BER can achieve to be below the 20% SD-FEC limit when ROP is greater than approximately -6.8 dBm. Additionally, BER of the 100Gbit/s IM/DD optical multi-rate Nyquist-SCM system using PCS QAM modulation scheme is below 7% HD-FEC limit with the ROP great than approximately -4.5 dBm.

To predict post-FEC BER performance, NGMI is more commonly used than the pre-FEC BER for systems adopting PCS QAM, which can be estimated as [26], [27]

$$\text{NGMI} \approx 1 - \frac{1}{mS} \sum_{k=1}^S \sum_{i=1}^m \log_2 \left(1 + e^{(-1)^{b_{k,i}} \Lambda_{k,i}} \right) \quad (14)$$

where $m = \log_2(M)$ and S is the number of symbols. $b_{k,i}$ is the transmitted bits and $\Lambda_{k,i}$ represents the log-likelihood

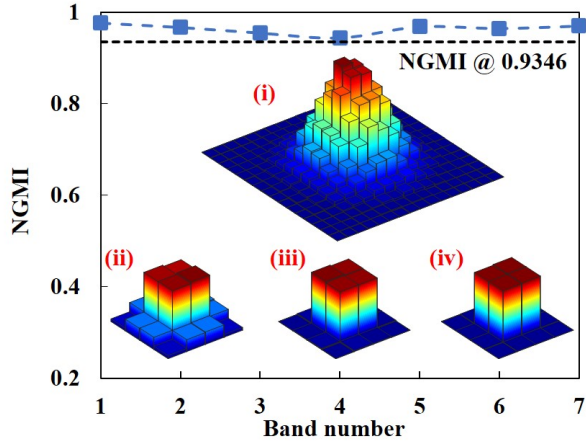


Fig. 8. NGMI of 100Gbit/s IM/DD optical multi-rate Nyquist-SCM each band signal adopting PCS QAM over 50km SSMF transmission at ROP of approximately -4 dBm. Insets are the probability of the constellation points of the (i) 1st, (ii) 3rd, (iii) 5th and (iv) 7th band, respectively.

ratio. The FEC overhead (OH) can be predicted by [28]

$$\text{OH} = (1 - \text{NGMI})/\text{NGMI}. \quad (15)$$

The corresponding NGMI threshold of 7% FEC OH is about 0.9346. Fig. 8 shows the NGMI of each band of 100Gbit/s IM/DD optical multi-rate Nyquist-SCM system adopting PCS QAM over 50km SSMF transmission at ROP of approximately -4 dBm. NGMIs of each band are larger than 0.9346, which implies that the 7% FEC OH is enough for decoding. Insets show the probability of the constellation points of the (i) 1st, (ii) 3rd, (iii) 5th and (iv) 7th band, respectively. They are similar with those shown in Fig. 4.

The average NGMI is important for the multi-carriers system for the reason that channel coding and decoding are performed to the data of all carriers together. Average NGMI of such multi-rate SCM system can be calculated as [29]

$$\text{NGMI}_{\text{ave}} = \frac{\sum_{i=1}^N RS_i \times m_i \times \text{NGMI}_i}{\sum_{i=1}^N RS_i \times m_i}. \quad (16)$$

When 20% low density parity check with 6.25% staircase code is considered as the FEC code, the NGMI should be larger than 0.858 to achieve the 10^{-15} post-FEC BER [30]. Fig. 9 shows the average NGMI versus ROPs for 100Gbit/s IM/DD optical multi-rate Nyquist-SCM system adopting PCS QAM over OBTB and 50km SSMF transmission. For OBTB transmission scenario, when ROP are equal or greater than -10 dBm and -7 dBm, the average NGMIs are greater than the NGMI thresholds of 0.858 and 0.9346, respectively. For 50km SSMF transmission scenario, when ROP are equal or greater than -6 dBm and -4 dBm, the average NGMIs are greater than the NGMI thresholds of 0.858 and 0.9346, respectively. When ROP is approximately -4 dBm, the average NGMI is 0.967. Therefore, both pre-FEC BER and average NGMI indicate that the multi-rate Nyquist-SCM adopting PCS QAM scheme not only has a strong resistance to CD, but also makes full utilization of SNR to maximize the capacity-reach.

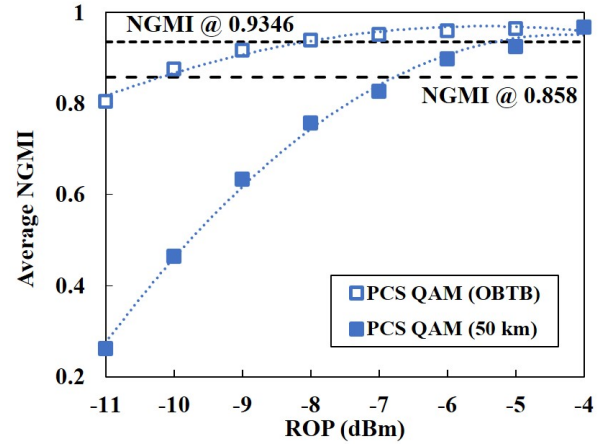


Fig. 9. The average NGMI versus ROPs for 100Gbit/s IM/DD optical multi-rate Nyquist-SCM system adopting PCS QAM over OBTB and 50km SSMF transmission.

V. CONCLUSION

In this paper, to the best of our knowledge, we propose the first multi-rate Nyquist-SCM for C-band 100Gbit/s signal transmission over 50km dispersion-uncompensated link. Based on the characteristics of dispersive channel, an optical DSB Nyquist-SCM with multi-rate subcarriers is proposed to keep away from the CD-caused spectral nulls flexibly. As a result, the multi-rate Nyquist-SCM signal has a strong resistance to CD. Signal of each subcarrier can be recovered individually by ACMD algorithm with an acceptable complexity, including the FFE with no more than 31 taps, a two-tap PF and MLSE with one memory length. Combining with entropy loading based on PCS to maximize the capacity-reach, the multi-rate Nyquist-SCM for C-band 100Gbit/s signal over 50km dispersion-uncompensated link achieves 7% HD-FEC limit and average NGMI of 0.967. In conclusion, the multi-rate Nyquist-SCM shows great potentials in solving the CD-caused spectral distortions, which successfully combines the advanced technologies of Nyquist-SCM, multi-rate subcarriers, ACMD algorithm and entropy loading based on PCS.

REFERENCES

- [1] X. Zhou, R. Urata, and H. Liu, "Beyond 1Tb/s datacenter interconnect technology: challenges and solutions," in *Optical Fiber Communications Conference and Exhibition (OFC)*. Optical Society of America, 2019, p. Tu2F.5.
- [2] K. Zhong, X. Zhou, J. Huo, C. Yu, C. Lu, and A. P. T. Lau, "Digital signal processing for short-reach optical communications: A review of current technologies and future trends," *Journal of Lightwave Technology*, vol. 36, no. 2, pp. 377–400, 2018.
- [3] Q. Cheng, M. Bahadori, M. Glick, S. Rumley, and K. Bergman, "Recent advances in optical technologies for data centers: a review," *Optica*, vol. 5, no. 11, pp. 1354–1370, 2018.
- [4] G. N. Liu, L. Zhang, T. Zuo, and Q. Zhang, "IM/DD transmission techniques for emerging 5G fronthaul, DCI, and metro applications," *Journal of Lightwave Technology*, vol. 36, no. 2, pp. 560–567, 2018.
- [5] M. Chagnon, "Direct-detection technologies for intra-and inter-data center optical links," in *2019 Optical Fiber Communications Conference and Exhibition (OFC)*. Optical Society of America, 2019, p. W1F.4.
- [6] J. Wei, Q. Zhang, L. Zhang, N. Stojanovic, C. Prodaniuc, F. Karinou, and C. Xie, "Challenges and advances of direct detection systems for DCI and metro networks," in *2018 Optical Fiber Communications Conference and Exposition (OFC)*. Optical Society of America, 2018, p. W2A.60.

- [7] Y. Hong, K. R. Bottrill, N. Taengnoi, N. K. Thipparapu, Y. Wang, J. K. Sahu, D. J. Richardson, and P. Petropoulos, "Numerical and experimental study on the impact of chromatic dispersion on O-band direct-detection transmission," *Applied Optics*, vol. 60, no. 15, pp. 4383–4390, 2021.
- [8] N. Eiselt, J. Wei, H. Griesser, A. Dochhan, M. H. Eiselt, J.-P. Elbers, J. J. V. Olmos, and I. T. Monroy, "Evaluation of real-time 8×56.25 Gb/s (400G) PAM-4 for inter-data center application over 80 km of SSMF at 1550 nm," *Journal of Lightwave Technology*, vol. 35, no. 4, pp. 955–962, 2016.
- [9] J. Zhang, J. Yu, and H.-C. Chien, "EML-based IM/DD 400G (4×112.5 -Gbit/s) PAM-4 over 80 km SSMF based on linear pre-equalization and nonlinear LUT pre-distortion for inter-DCI applications," in *2017 Optical Fiber Communications Conference and Exhibition (OFC)*. Optical Society of America, 2017, p. W4I.4.
- [10] Q. Zhang, N. Stojanovic, T. Zuo, L. Zhang, C. Prodaniuc, F. Karinou, C. Xie, and E. Zhou, "Single-lane 180 Gb/s SSB-duobinary-PAM-4 signal transmission over 13 km SSMF," in *Optical Fiber Communication Conference*. Optical Society of America, 2017, p. Tu2D.2.
- [11] Q. Zhang, N. Stojanovic, C. Xie, C. Prodaniuc, and P. Laskowski, "Transmission of single lane 128 Gbit/s PAM-4 signals over an 80 km SSMF link, enabled by DDMZM aided dispersion pre-compensation," *Optics Express*, vol. 24, no. 21, pp. 24 580–24 591, 2016.
- [12] J. Wei, N. Stojanovic, and C. Xie, "Nonlinearity mitigation of intensity modulation and coherent detection systems," *Optics Letters*, vol. 43, no. 13, pp. 3148–3151, 2018.
- [13] X. Tang, S. Liu, Z. Sun, H. Cui, X. Xu, J. Qi, M. Guo, Y. Lu, and Y. Qiao, "C-band 56-Gb/s PAM4 transmission over 80-km SSMF with electrical equalization at receiver," *Optics Express*, vol. 27, no. 18, pp. 25 708–25 717, 2019.
- [14] R. Rath, D. Clausen, S. Ohlendorf, S. Pachnicke, and W. Rosenkranz, "Tomlinson–Harashima precoding for dispersion uncompensated PAM-4 transmission with direct-detection," *Journal of Lightwave Technology*, vol. 35, no. 18, pp. 3909–3917, 2017.
- [15] J. Zhou, H. Wang, L. Liu, C. Yu, Y. Feng, S. Gao, W. Liu, and Z. Li, "C-band 56 Gbit/s on/off keying system over a 100 km dispersion-uncompensated link using only receiver-side digital signal processing," *Optics Letters*, vol. 45, no. 3, pp. 758–761, 2020.
- [16] J. Zhou, H. Wang, Y. Feng, W. Liu, S. Gao, C. Yu, and Z. Li, "Processing for dispersive intensity-modulation and direct-detection fiber-optic communications," *Optics Letters*, vol. 46, no. 1, pp. 138–141, 2021.
- [17] L. Nadal, M. S. Moreolo, J. M. Fàbrega, A. Dochhan, H. Grießer, M. Eiselt, and J.-P. Elbers, "DMT modulation with adaptive loading for high bit rate transmission over directly detected optical channels," *Journal of Lightwave Technology*, vol. 32, no. 21, pp. 3541–3551, 2014.
- [18] S. T. Le, T. Drenski, A. Hills, M. King, K. Kim, Y. Matsui, and T. Sizer, "100Gbps DMT ASIC for Hybrid LTE-5G Mobile Fronthaul Networks," *Journal of Lightwave Technology*, vol. 39, no. 3, pp. 801–812, 2021.
- [19] Z. Li, M. S. Erkilinc, K. Shi, E. Sillekens, L. Galdino, T. Xu, B. C. Thomsen, P. Bayvel, and R. I. Killely, "Spectrally efficient 168 Gb/s/ λ WDM 64-QAM single-sideband Nyquist-subcarrier modulation with Kramers–Kronig direct-detection receivers," *Journal of Lightwave Technology*, vol. 36, no. 6, pp. 1340–1346, 2018.
- [20] M. S. Erkilinc, S. Pachnicke, H. Griesser, B. C. Thomsen, P. Bayvel, and R. I. Killely, "Performance comparison of single-sideband direct detection Nyquist-subcarrier modulation and OFDM," *Journal of Lightwave Technology*, vol. 33, no. 10, pp. 2038–2046, 2015.
- [21] H. Wang, J. Zhou, D. Guo, Y. Feng, W. Liu, C. Yu, and Z. Li, "Adaptive Channel-Matched Detection for C-Band 64-Gbit/s Optical OOK System Over 100-km Dispersion-Uncompensated Link," *Journal of Lightwave Technology*, vol. 38, no. 18, pp. 5048–5055, 2020.
- [22] H. Sun, M. Torbatian, M. Karimi, R. Maher, S. Thomson, M. Tehrani, Y. Gao, A. Kumpera, G. Soliman, A. Kakkar *et al.*, "800G DSP ASIC design using probabilistic shaping and digital sub-carrier multiplexing," *Journal of lightwave technology*, vol. 38, no. 17, pp. 4744–4756, 2020.
- [23] J. Zhou, L. Zhang, T. Zuo, Q. Zhang, S. Zhang, E. Zhou, and G. N. Liu, "Transmission of 100-Gb/s DSB-DMT over 80-km SMF Using 10-G class TTA and Direct-Detection," in *ECOC 2016; 42nd European Conference on Optical Communication*. VDE, 2016, p. Tu.3.F.1.
- [24] J. Zhou, C. Yang, D. Wang, Q. Sui, H. Wang, S. Gao, Y.-H. Feng, W. Liu, Y. Yan, J. Li *et al.*, "Burst-Error-Propagation Suppression for Decision-Feedback Equalizer in Field-Trial Submarine Fiber-Optic Communications," *Journal of Lightwave Technology*, 2021.
- [25] J. Wei and E. Giacomidis, "Multi-band CAP for next-generation optical access networks using 10-G optics," *Journal of Lightwave Technology*, vol. 36, no. 2, pp. 551–559, 2017.
- [26] J. Cho, L. Schmalen, and P. J. Winzer, "Normalized generalized mutual information as a forward error correction threshold for probabilistically shaped QAM," in *2017 European Conference on Optical Communication (ECOC)*. IEEE, 2017, p. M.2.D.2.
- [27] X. Chen, Y. Chen, M. Tang, T. Tong, S. Fu, and D. Liu, "Adaptive Uniform Entropy Loading for SSB-DMT Systems," *Journal of Lightwave Technology*, vol. 37, no. 23, pp. 5961–5970, 2019.
- [28] D. Che and W. Shieh, "Squeezing out the last few bits from band-limited channels with entropy loading," *Optics Express*, vol. 27, no. 7, pp. 9321–9329, 2019.
- [29] X. Chen, S. Chandrasekhar, J. Cho, and P. Winzer, "Single-wavelength and single-photodiode entropy-loaded 554-Gb/s transmission over 22-km SMF," in *Optical Fiber Communication Conference*. Optical Society of America, 2019, p. Th4B.5.
- [30] A. Alvarado, E. Agrell, D. Lavery, R. Maher, and P. Bayvel, "Replacing the soft-decision FEC limit paradigm in the design of optical communication systems," *Journal of Lightwave Technology*, vol. 33, no. 20, pp. 4338–4352, 2015.